Calculation of critical dimensions for wurtzite and cubic zinc blende coaxial nanowire heterostructures

S. Raychaudhuri and E. T. Yu[a)]
Department of Electrical and Computer Engineering,University of California, San Diego, La Jolla, California 92093-0407

(Received 15 January 2006; accepted 23 February 2006; published 25 July 2006)

We employ a methodology, based on established approaches for determining the critical thickness for strain relaxation in planar films, to determine critical dimensions for coherently strained coaxial nanowire heterostructures. The model is developed and executed for various specific core-shell heterostructures in [111] zinc blende and [0001] wurtzite geometries. These calculations reveal that critical dimensions in such heterostructures can be quantified by a unique critical core radius and a critical shell thickness, which is dependent on the core radius. It is anticipated that this work will serve as a guide to determine the feasibility of specific coherently strained nanowire heterostructure designs. © *2006 American Vacuum Society.* [DOI: 10.1116/1.2216715]

I. INTRODUCTION

Recent successes in the growth and fabrication of semiconductor nanowires[1,2] have led to opportunities in device design for a variety of applications, including chemical and biological sensors,[3] field effect transistors,[4,5] laser diodes,[6,7] and light emitting diodes.[8,9] Many of these devices either require or can benefit from the use of heterostructures in their design, and nanowire heterostructures in both coaxial[5] and axial[10] geometries have been proposed to optimize device performance. In determining the feasibility of these designs, it is necessary to consider the strain that arises in heterostructures due to the lattice mismatch between materials. Such strain not only affects the electronic and optical properties of the device but also determines the device dimensions at which coherence is lost and dislocations form, which will significantly alter or degrade device performance. Furthermore, the types of dislocations or other defects by which relaxation occurs will vary between crystal structures mandating analysis specific to each possible crystal structure.

Only a limited amount of work has been done previously to model coherence and critical dimensions in nanowire structures. A model was developed recently to describe strain and coherence in axial nanowire heterostructures,[11] while the critical dimensions of isotropic coaxial structures[12] have been estimated by comparing the strain energy of two discrete states of the system. In a recent paper[13] we presented a methodology for determining coherent geometries in coaxial nanowire heterostructures based on the formalism commonly used in thin film heteroepitaxy[14,15] and used it to determine the coherency limits in specific wurtzite nanowire systems. In this article we extend this methodology to explore and contrast coherency limits in both wurtzite and zinc blende structures. The results of these explorations are expected to serve as a guide to determine the feasibility of various core-shell device structures.

[a)]Electronic mail: ety@ece.ucsd.edu

II. ANALYTICAL FRAMEWORK

The geometry of the nanowire system considered is shown in Fig. 1. The nanowire consists of a core material of radius r and shell material of thickness h. The axis of the wire is assumed to be along the [111] direction for zinc blende structures and along the [0001] direction for wurtzite structures. In both cases the coherence requirement between the core and shell will result in cross-sectional and longitudinal strain components due to the mismatch in lattice parameters along the length of the wire as well as around the cylindrical surface of the wire.

In this analysis we are interested in determining the geometric limits at which coherence is lost in an analytical fashion that provides intuitive guidance and can be easily translated between material systems. A commonly used methodology to predict coherency limits in planar structures examines the strain energy of the system and determines the film thickness at which it becomes energetically favorable to relieve lattice strain by inserting a dislocation.[14,15] We will employ a similar approach to determine the coherency limits of the coaxial nanowire heterostructure.[13] We first solve for the lattice mismatch strain energy in the system, then determine the energetics associated with dislocations that are likely to form, and finally, determine the geometric limits at which it becomes favorable for these dislocations to appear. This analysis considers only strain energies due to lattice mismatch and dislocations and does not take into account the effects of faceting or other surface energy effects. For sufficiently large structures these effects are not expected to significantly alter the outcome of the calculation. For smaller structures where these effects could contribute more significantly to strain relaxation behavior, the analytical approach presented here must be supplemented by a much more detailed and likely numerical approach.

In general it is found that the nanowire geometry is more forgiving than its thin film counterpart in that a number of dimensional choices exist to attain a stable coherent structure. For a given choice of materials and alloy compositions, there exists a critical core radius, below which the structure

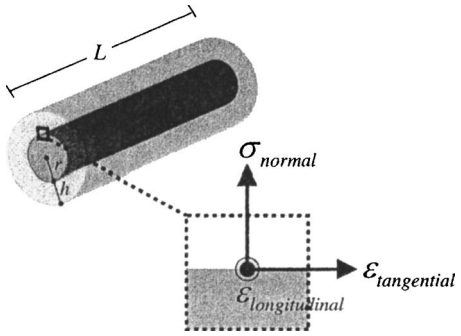

FIG. 1. Diagram of the relevant geometric parameters for a coaxial nanowire heterostructure as well as stress (σ) and strain (ε) boundary constraints for a single point on the coaxial heterointerface.

is always coherent regardless of shell thickness. Structures with a core radius greater than this critical value can still be stable provided that the shell thickness is below a critical shell thickness value. The critical shell thickness is dependent on the core radius and will vary depending on the material system being considered. The critical dimensions are found to be dependent only on core radius and shell thickness and have no dependence on the length of the wire.

A. Coherent strain energy calculation

A detailed treatment of how to calculate lattice mismatch strain energy in a coherently strained coaxial heterostructure is presented in Ref. 13. The basic methodology assumes that planar boundary conditions can be assigned to a single point on the heterointerface. As shown in Fig. 1, for a single point on the interface it is possible to define two perpendicular strain components due to lattice mismatch, one along the length of the wire ($\varepsilon_{\text{longitudinal}}$) and the other tangential to the heterointerface ($\varepsilon_{\text{tangential}}$). Because the radius of the wire is free to expand or contract to accommodate strain, the stress normal to a given point on the interface (σ_{normal}) is taken to be zero. By applying these boundary constraints, it is possible to solve for the full strain field at a single point on the interface using well-known relations between stress and strain.[16] This approach can then be used at each point on the heterointerface to obtain an expression for the total strain energy in the system. The coherent strain energies in the core and shell regions are found to be a function of the region geometry, the strain boundary constraints imposed on the region, and the elastic stiffness tensor of the material within the region.

1. Coherent strain energy in zinc blende nanowire structure

In order to use this methodology to calculate the coherent strain energy in [111] zinc blende coaxial nanowire structures, it is necessary to define an appropriately oriented elastic stiffness matrix c_{ij} and proper longitudinal and tangential lattice mismatch boundary conditions. Because the zinc blende nanowire is assumed to be oriented along the [111] direction, it is necessary to rotate c_{ij} such that the z axis of c_{ij} is parallel to the [111] direction. This must be done in order to make sure that the normal, tangential, and longitudinal boundary constraints are oriented properly with respect to the crystal structure. The coherent strain energy expressions for the core and shell regions of a zinc blende nanowire are then given by

$$U_{\text{ZB}}^{(i)} = \frac{A^{(i)}(f_l^{(i)})^2 + B^{(i)} f_l^{(i)} f_t^{(i)} + C^{(i)}(f_t^{(i)})^2}{D^{(i)}} L\pi[r^2], \tag{1}$$

$$U_{\text{ZB}}^{(ii)} = \frac{A^{(ii)}(f_l^{(ii)})^2 + B^{(ii)} f_l^{(ii)} f_t^{(ii)} + C^{(ii)}(f_t^{(ii)})^2}{D^{(ii)}} L\pi[(r+h)^2 - r^2], \tag{2}$$

respectively, where f_t and f_l represent the tangential and longitudinal strain constraints, A, B, C, and D are given by

$$A = {c_{11}}^2 - 2{c_{12}}^2 + 40c_{12}c_{44} + 16{c_{44}}^2 + c_{11}(c_{12} + 26c_{44}), \tag{3}$$

$$B = 4(c_{11} - 2c_{12} - 2c_{44})(c_{11} - c_{12} + 4c_{44}), \tag{4}$$

$$C = 4(c_{11} + 2c_{12} + c_{44})(c_{11} - c_{12} + 4c_{44}), \tag{5}$$

$$D = 18(c_{11} + c_{12} + 2c_{44}), \tag{6}$$

and variables with superscripts (i) and (ii) denote parameters specific to the core and shell materials, respectively.

In zinc blende structures the tangential and longitudinal lattice strain boundary conditions in the core and the shell are given by

$$f_t^{(i)} = \frac{a - a^{(i)}}{a^{(i)}}, \tag{7}$$

$$f_t^{(ii)} = \frac{a - a^{(ii)}}{a^{(ii)}}, \tag{8}$$

$$f_l^{(i)} = \frac{a - a^{(i)}}{a^{(i)}}, \tag{9}$$

$$f_l^{(ii)} = \frac{a - a^{(ii)}}{a^{(ii)}}, \tag{10}$$

where a represents the strained cubic lattice constant of the system, $a^{(i)}$ represents the unstrained lattice parameter of the core material, and $a^{(ii)}$ represents the unstrained lattice parameter of the shell material. For a given geometry and material composition the equilibrium lattice constant a will assume a value that minimizes the total strain energy of the system. By minimizing $U_{\text{strain}} = U^{(i)} + U^{(ii)}$, the equilibrium lattice strain is found to be

$$a = \frac{a^{(ii)}a^{(i)}(a^{(ii)}r^2\chi^{(i)} + a^{(i)}h(h+2r)\chi^{(ii)})}{a^{(ii)}r^2\chi^{(i)} + {a^{(i)}}^2 h(h+2r)\chi^{(ii)}}, \tag{11}$$

where $\chi^{(i)}$ and $\chi^{(ii)}$ are given by

$$\chi_{\text{zinc blende}} = \frac{(c_{11}+2c_{12})(c_{11}-c_{12}+6c_{44})}{2(c_{11}+c_{12}+2c_{44})}. \quad (12)$$

The equilibrium lattice constant value falls somewhere between the relaxed core and shell values and will tend toward that of the region with greater volume. This is expected given the direct relationship between strain energy and volume seen in Eqs. (1) and (2). This result shows that for a given choice of material, geometry will determine the distribution of lattice strain between the core and shell materials. It is because of this that the dimensions of both core and shell must be considered in determining stable coherent geometries.

2. Coherent strain energy in wurtzite nanowire structures

Using a similar approach, the coherent strain energy expressions for the core and shell regions of a wurtzite nanowire are found to be[13]

$$U_W^{(i)} = \frac{(c_{11}^{(i)}f_t^{(i)})^2 - (c_{12}^{(i)}f_t^{(i)} + c_{13}^{(i)}f_l^{(i)})^2 + c_{11}^{(i)}f_l^{(i)}(c_{13}^{(i)}f_t^{(i)} + c_{33}^{(i)}f_l^{(i)})^2}{2c_{11}^{(i)}} L\pi[r^2], \quad (13)$$

$$U_W^{(ii)} = \frac{(c_{11}^{(ii)}f_t^{(ii)})^2 - (c_{12}^{(ii)}f_t^{(ii)} + c_{13}^{(ii)}f_l^{(ii)})^2 + c_{11}^{(ii)}f_l^{(ii)}(c_{13}^{(ii)}f_t^{(ii)} + c_{33}^{(ii)}f_l^{(ii)})^2}{2c_{11}^{(ii)}} L\pi[(r+h)^2 - r^2]. \quad (14)$$

In wurtzite structures the tangential and longitudinal lattice strain constraints are determined by the mismatch in the a and c lattice parameters, respectively. The tangential strain boundary conditions in the core and the shell are given by

$$f_t^{(i)} = \frac{a - a^{(i)}}{a^{(i)}}, \quad (15)$$

$$f_t^{(ii)} = \frac{a - a^{(ii)}}{a^{(ii)}}, \quad (16)$$

and the longitudinal strain boundary conditions in the core and shell are given by

$$f_l^{(i)} = \frac{c - c^{(i)}}{c^{(i)}}, \quad (17)$$

$$f_l^{(ii)} = \frac{c - c^{(ii)}}{c^{(ii)}}, \quad (18)$$

where a and c represent the strained lattice constants of the system, $a^{(i)}$ and $c^{(i)}$ represent the unstrained lattice parameters of the core material, and $a^{(ii)}$ and $c^{(ii)}$ represent the unstrained lattice parameters of the shell material. The equilibrium lattice constants in wurtzite structures exhibit a similar geometric dependence as in the zinc blende case.[13] As a result both a and c can be computed using Eq. (11) after substituting

$$\chi_{\text{wurtzile}} = \frac{{c_{11}}^2 - (c_{12}+c_{13})^2 + c_{11}(2c_{13}+c_{33})}{2c_{11}} \quad (19)$$

for $\chi^{(i)}$ and $\chi^{(ii)}$.

B. Partial relaxation through dislocation formation

The insertion of an edge dislocation at the core-shell interface can allow partial relaxation of lattice mismatch strain but will also contribute a strain field associated with the dislocation itself. In order to determine the energetics associated with these phenomena, it is necessary first to identify the types of dislocations that are likely to form in the system being considered. This can be done by considering dislocations known to be stable in a given crystal structure along with dislocation orientations that will relieve lattice strain.

1. Dislocations in zinc blende nanowires

Perfect dislocations in zinc blende structures tend to be either pure screw or 60 mixed dislocations along the ⟨011⟩ directions.[17] For zinc blend nanowires grown along the [111] direction, it is not possible for a perfect dislocation to lie along the length of the nanowire as shown in Fig. 2(a). Thus

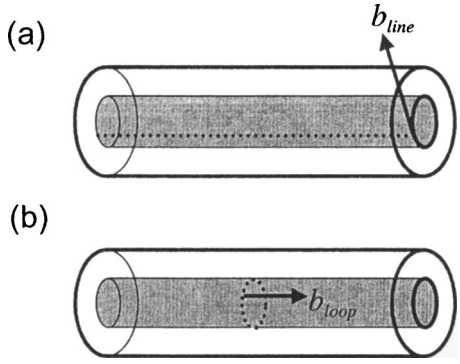

FIG. 2. (a) Orientation of an edge dislocation line along the axis of the wire with a Burgers vector, b_{line}, tangential to the circular heterointerface. (b) Orientation of an edge dislocation loop in the cross-sectional plane of the wire with Burgers vector, b_{loop}, along the length of the wire.

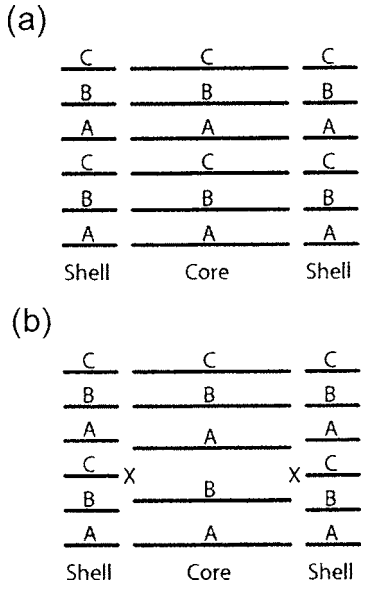

FIG. 3. (a) Stacking sequence of (111) planes in a coherently strained [111] zinc blende coaxial nanowire. (b) Stacking sequence of (111) planes in a [111] zinc blende nanowire with a stacking fault in the core region. The "X" represents the location of an edge dislocation loop formed around the core as a result of the stacking error.

this type of dislocation is not expected to define the critical dimensions in zinc blende structures.

The formation of a dislocation loop around the core of the nanowire, as shown in Fig. 2(b), could serve to relieve lattice strain along the length of the wire and has been observed in some coaxial nanowires heterostructures with zinc blende regions.[18] Such an edge dislocation loop could form as a result of a partial-stacking fault. Zinc blende wires oriented in the [111] direction are comprised of (111) planes of atoms stacked in an *ABC* sequence, as shown in Fig. 3(a). A stacking fault will either insert or remove a (111) plane of atoms in the core or shell of the structure, as shown in Fig. 3(b). This insertion or removal of a (111) plane will result in a two-dimensional dislocation in the region where the stacking fault has occurred but will also create an edge dislocation loop[17] around the core region of the heterostructure, such as the one shown in Fig. 2(b). The magnitude and orientation of the Burgers vector of such a loop will efficiently relieve longitudinal strain, and the loop is thus expected to be the type of dislocation that will define the critical dimensions in zinc blende coaxial heterostructures.

When calculating the energy associated with such a dislocation, it is necessary to consider the strain energy associated with the partial edge dislocation loop about the core as well as the energy due to the stacking fault. The total energy associated with this type of dislocation is[17]

$$U_{\text{loop}} = n_{\text{loop}} L \left(2\pi r \frac{1}{6} (c_{11}^{(ii)} - c_{12}^{(ii)} + 4c_{44}^{(ii)}) \frac{{b_{\text{loop}}}^2}{4\pi} \times \log\left[\frac{32r}{b_{\text{loop}}} - 1 \right] + \gamma A_{\text{fault}} \right), \tag{20}$$

where n_{loop} refers to the dislocation loop density per unit length along the axis of the wire, b_{loop} refers to the magnitude of the Burgers vector, γ is the stacking fault energy per unit area, and A_{fault} is the area of the stacking fault. Although the strain field generated by the dislocation will exist in both the core and shell materials, c_{ij} values are arbitrarily chosen to be those of the shell; this is reasonable since in most viable heterojunction material systems, $c_{ij}^{(i)}$ and $c_{ij}^{(ii)}$ are sufficiently similar that the choice between them will not significantly impact the final calculation. The value of b_{loop} is expected to be $a/\sqrt{3}$ for this type of dislocation[17] and A_{fault} will be the cross-sectional area of the core or the shell depending on the region in which the stacking error has occurred. It should be noted that Eq. (20) is derived for a dislocation loop in an infinite medium, but because the expression assumes that the loop terminates its own strain field, it should produce a reasonable estimate for the strain energy in sufficiently large coaxial nanowire structures.

In examining the energetics of a dislocation at the interface, it is necessary to consider not only the strain energy associated with the dislocation itself but also the lattice relaxation that is expected to occur with the inclusion of a dislocation. For planar thin films grown on bulk substrates, the one-dimensional lattice strain including relaxation due to dislocation formation is given by[15]

$$f_{\text{film}} = \frac{a_{\text{substrate}} - a_{\text{film}}}{a_{\text{film}}} - nb, \tag{21}$$

where $a_{\text{substrate}}$ represents the strained lattice constant of the film, a_{film} represents the relaxed lattice constant of the film, n refers to the line dislocation density per unit length, and b refers to the edge component of the dislocation Burgers vector. The lattice relaxation term nb accounts for the film relaxation due to the formation of dislocations at the heterointerface. The system described by Eq. (21) assumes that all strain will be in the film, and thus only relaxation in the film is considered.

In the case of the coaxial nanowire structures, strain will be distributed between the core and the shell. The formation of an edge dislocation at the interface will result in the insertion or removal of a plane of atoms in the system. This will change the strain constraint in both core and shell materials since the two are interdependent. Because the system will tend to minimize total strain energy in the system, the region experiencing the greater lattice mismatch will receive the bulk of the lattice relaxation that occurs. It is therefore necessary to distribute the lattice relaxation term between the core and shell while incorporating it into the lattice strain expressions. The lattice mismatch strain expressions are then given by

$$f_l^{(i)} = \frac{a - a^{(i)}}{a^{(i)}} - \left(\frac{a^{(i)} - a}{|a^{(i)} - a^{(ii)}|} \right) n_{\text{loop}} b_{\text{loop}}, \tag{22}$$

$$f_l^{(ii)} = \frac{a - a^{(ii)}}{a^{(ii)}} - \left(\frac{a - a^{(ii)}}{|a^{(i)} - a^{(ii)}|} \right) n_{\text{loop}} b_{\text{loop}}. \tag{23}$$

These expressions resemble Eq. (21) except that the lattice relaxation term is now divided between the core and shell.

Equations (22) and (23) model the effect described above by using the equilibrium lattice constant and the relaxed lattice constant values to apportion the relaxation term such that the total strain energy in the system is minimized. Numerical computations were carried out to minimize the total energy in the system with respect to the division of the strain relaxation term. The results of these calculations were found to be nearly identical to the functions used in Eqs. (22) and (23), confirming that the equilibrium lattice constant can be used to estimate the distribution of strain relaxation between the core and shell.

2. Dislocations in wurtzite nanowires

In contrast to the zinc blende case, wurtzite coaxial nanowire heterostructures are expected to relax through the formation of a pure edge dislocation along the length of the wire as shown in Fig. 2(a).[13] Such a dislocation will relieve strain in the cross section of the nanowire. The strain energy associated with this type of dislocation is[17]

$$U_{\text{line}} = n_{\text{line}} 2\pi r L \left(\frac{c_{11}^{(ii)} - c_{12}^{(ii)}}{2c_{11}^{(ii)}} \right) \frac{b_{\text{line}}^2}{4\pi} \log\left[\frac{4h}{b_{\text{line}}} \right], \tag{24}$$

where n_{line} refers to the dislocation line density per unit length about the circumference of the heterointerface and b_{line} refers to the magnitude of the Burgers vector for such a dislocation. In this expression the dislocation is assumed to be located at the heterointerface, as shown in Fig. 2(a), and the strain field is assumed to terminate at the free surface of the nanowire system. This is analogous to the approach used for computing dislocation energies when calculating critical thickness in planar heterostructures.[14,15] The value of b_{line} is expected to be that of the equilibrium lattice constant a.[19]

The formation of a such a line dislocation will allow for the partial relaxation of tangential lattice mismatch strain by inserting or removing a plane of atoms. As in the zinc blende case, the resulting relaxation in lattice strain will be distributed between the core and shell materials such that total strain energy in the system is minimized. Applying the same model to distribute the relaxation term as used in the zinc blende case, the tangential strain elements become

$$f_t^{(i)} = \frac{a - a^{(i)}}{a^{(i)}} - \left(\frac{a^{(i)} - a}{|a^{(i)} - a^{(ii)}|} \right) n_{\text{line}} b_{\text{line}}, \tag{25}$$

$$f_t^{(ii)} = \frac{a - a^{(ii)}}{a^{(ii)}} - \left(\frac{a - a^{(ii)}}{|a^{(i)} - a^{(ii)}|} \right) n_{\text{line}} b_{\text{line}}. \tag{26}$$

for the core and shell regions, respectively.

C. Critical geometry calculation

The total strain energy in the system is the sum of the lattice mismatch strain energy in the core and shell regions as well as the energy due to the presence of the dislocations discussed above. The expressions for the total strain energy for zinc blende and wurtzite structures including dislocations are

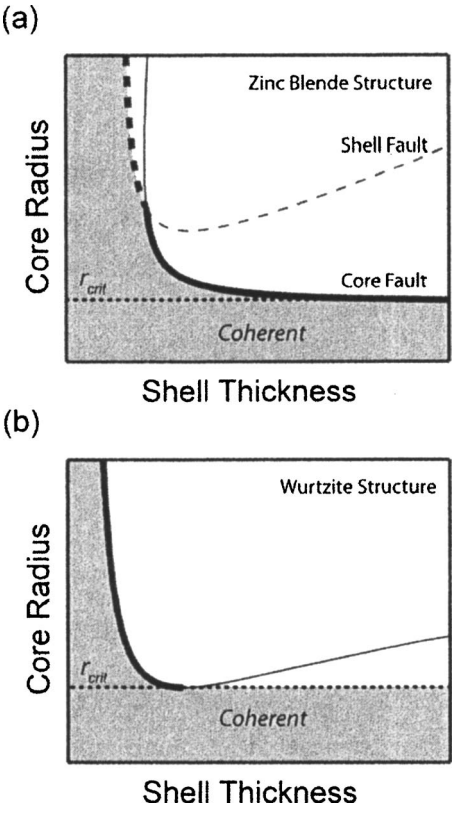

FIG. 4. Schematic plot of the critical dimensions for a (a) zinc blende and (b) wurtzite coaxial nanowire structure. The shaded region of the plots shows all possible strained coherent geometries, which are quantified by the critical core radius r_{crit} and the critical shell thickness curve (darkened portion of the curves).

$$U_{\text{tot}} = U_{\text{ZB}}^{(i)} + U_{\text{ZB}}^{(ii)} + U_{\text{loop}}, \tag{27}$$

$$U_{\text{tot}} = U_{W}^{(i)} + U_{W}^{(ii)} + U_{\text{line}}, \tag{28}$$

respectively, where $U_{\text{ZB}}^{(i)}$ and $U_{\text{ZB}}^{(ii)}$ are calculated using Eqs. (7) and (8) and Eqs. (22) and (23) and $U_{W}^{(i)}$ and $U_{W}^{(ii)}$ are calculated using Eqs. (17) and (18) and Eqs. (25) and (26). The critical dimensions are obtained by determining the geometric limits at which it becomes energetically favorable to include a dislocation. This is done mathematically by evaluating $\partial U_{\text{tot}} / \partial n|_{n=0}$ and determining the dimensions for which this function changes from positive to negative.[15]

Such an analysis will determine the dimensions at which sufficient strain energy will be relieved by the insertion of a single dislocation to make up for the energy cost of inserting the dislocation. However, it does not take into account the energetic effects of interactions between dislocations, which are expected to be significant for nanoscale structures, and thus is only valid at the critical dimensions at which the first dislocation forms.

III. RESULTS AND DISCUSSION

Figure 4 shows a schematic plot indicating the general form of the results of the critical dimension calculation obtained for a specific wurtzite and zinc blende structure. The shaded portions of the plots show the combinations of core-

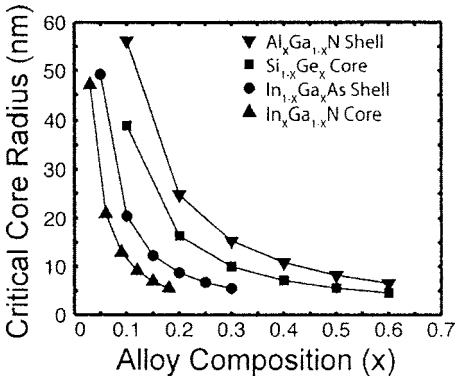

FIG. 5. Plot of the calculated critical core radius for various nanowire heterostructures as a function of alloy composition. The structures considered are comprised of an InAs core with an $In_{1-x}Ga_xAs$ shell (●), $Si_{1-x}Ge_x$ core with a Si shell (■), GaN core with an $Al_xGa_{1-x}N$ shell (▼), and $In_xGa_{1-x}N$ core with a GaN shell (▲).

shell dimensions that will yield coherently strained structures for a particular choice of material and alloy composition. More detailed calculation results for specific structures will be shown in Figs. 5–7.

The curves in Fig. 4 show the limiting geometries for dislocation formation. The solid and dashed curves in Fig. 4(a) show the limiting dimensions for the formation of a stacking fault in the core and shell regions of a zinc blende nanowire, respectively. The solid curve in Fig. 4(b) shows the limiting dimensions for the formation of a dislocation line in a wurtzite nanowire. From Figs. 4(a) and 4(b) we see that for a given combination of materials forming the coaxial nanowire heterostructure, there is a critical core radius r_{crit} below which the coaxial nanowire will be coherent regardless of shell thickness. Such a critical core radius exists because of the coaxial nanowire structure's ability to distribute strain between the core and shell. As the shell thickness increases eventually, all of the strain is passed to the core. Since the core volume is constant, the strain energy of the system will no longer change with shell thickness. If the core volume is sufficiently small, then the strain energy stored in the core will never be great enough to warrant the formation of a dislocation.

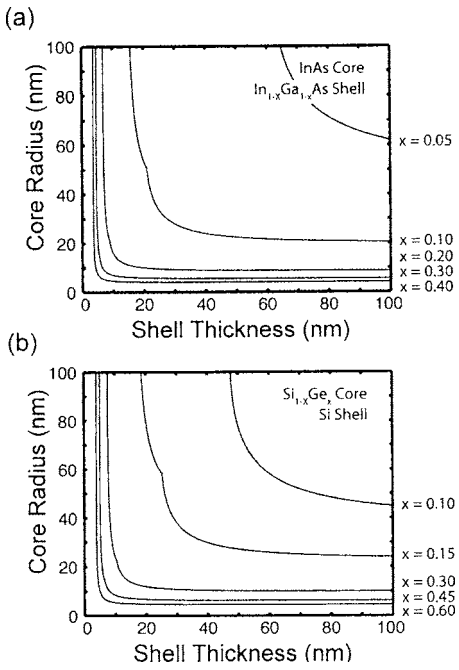

FIG. 6. Calculated critical dimensions for various zinc blende nanowire heterojunctions comprised of (a) InAs cores with $In_{1-x}Ga_xAs$ shells and (b) $Si_{1-x}Ge_x$ cores with Si shells.

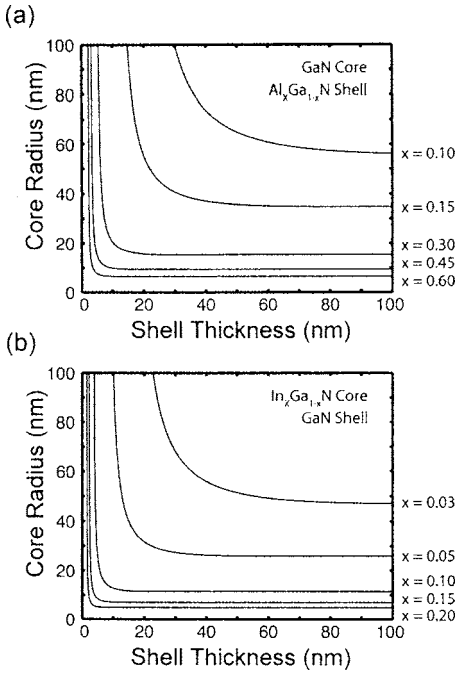

FIG. 7. Calculated critical dimensions for various wurtzite nanowire heterojunctions comprised of (a) GaN cores with $Al_xGa_{1-x}N$ shells and (b) $In_xGa_{1-x}N$ core with GaN shells.

The darker portions of the curves in Fig. 4(a) define a critical shell thickness for zinc blende structures with a core radius larger than the critical core radius. This critical shell thickness represents the shell thickness at which it becomes energetically favorable for a stacking fault to form. From Fig. 4(a) it is clear that at core radius values close to r_{crit}, the critical shell thickness will be limited by the formation of a stacking fault in the core region. As the core radius increases, however, the coherence limit will be defined by the formation of a stacking fault in the shell region. This occurs because the energy associated with a stacking fault in the core region increases more rapidly with core radius than the energy associated with a stacking fault in the shell region.

The darker portion of the curve in Fig. 4(b) defines a critical shell thickness for wurtzite structures with core radius larger than the critical core radius value. This critical shell thickness represents the shell thickness value at which it becomes energetically favorable to insert a line dislocation at the heterointerface for a given core radius. The positively sloped region of the dislocation curve (lighter portion of the curve) is a function of the assumption, used to calculate the dislocation strain energy U_{line}, that no other dislocations are

TABLE I. Relevant physical parameters for zinc blende materials.

	InAs	GaAs	Si	Ge	Reference
a (Å)	6.0583	5.6533	5.4310	5.6580	20
c_{11} (GPa)	83	119	160	124	20
c_{12} (GPa)	45	54	58	41	20
c_{44} (GPa)	40	60	80	68	20
γ (mJ/m^2)	30	45	55	60	21

present to terminate the dislocation strain field. Because a dislocation must have already formed in order to arrive at this region on the plot, the features of the curve in this region are not applicable in determining coherence. Though the mechanisms by which coherency is lost differ between zinc blende and wurtzite structures, Fig. 4 shows that in both cases the critical dimensions can be quantified by a critical core radius below which dislocations will never form and a critical shell thickness that is dependent on core radius.

Numerical calculations were carried out for a number of material systems as a function of alloy composition. Figure 5 shows the calculated critical core radii as a function of alloy composition for zinc blende structures comprised of InAs cores with $In_{x-1}Ga_xAs$ shells and $Si_{x-1}Ge_x$ cores with Si shells, as well as wurtzite structures comprised of GaN cores with $Al_xGa_{1-x}N$ shells and $In_xGa_{1-x}N$ cores with GaN shells. Figures 6(a), 6(b), 7(a), and 7(b) show the calculated critical dimensions for these structures, respectively. Each curve in Figs. 6 and 7 plots the combination of core radius and shell thickness at which the first dislocation is expected to form for a given alloy composition. Figures 5–7 were calculated using the material parameter values[20–22] listed in Tables I and II, all of which were assumed to vary linearly with alloy composition. Figures 5–7 suggest that the critical dimensions for reasonable alloy compositions are well within the range of experimental interest. In general these results show that there are a variety of compositional and geometric choices that will yield coherent structures, giving device designers a flexibility that is typically not observed in planar thin film devices.

IV. CONCLUSION

In summary, we have utilized a methodology, based on the well-known formalism used to determine the critical thickness in planar epitaxial growth, to determine coherent geometries for various zinc blende and wurtzite coaxial nanowire heterostructures. The unique geometry of the nanowire structure along with the volumetric similarity of the materials involved gives rise to a number of possible coherent structures for a given choice of materials and alloy compositions, which are quantified by a unique critical core radius and a critical shell thickness that is a function of the core radius. This flexibility is unique to nanowire structures and provides material and device engineers with increased flexibility in design not available in planar thin film heterostructures.

TABLE II. Relevant physical parameters for wurtzite materials.

	GaN	AIN	InN	Reference
a (Å)	3.199	3.110	3.585	22
c (Å)	5.227	4.995	5.801	22
c_{11} (GPa)	370	410	223	22
c_{12} (GPa)	145	140	115	22
c_{13} (GPa)	110	100	92	22
c_{33} (GPa)	390	390	224	22
c_{44} (GPa)	90	120	48	22

ACKNOWLEDGMENTS

Part of this work was supported by the National Science Foundation (NIRT ECS-05069). One of the authors (S.R.) acknowledges financial support from a Cal(IT)^2 fellowship.

[1] M. Law, J. Goldberger, and P. Yang, Annu. Rev. Mater. Res. **34**, 83 (2004).
[2] Y. W. Heo, D. P. Norton, L. C. Tien, Y. Kwon, B. S. Kang, F. Ren, S. J. Pearton, and J. R. LaRoche, Mater. Sci. Eng., R. **47**, 1 (2004).
[3] F. Patolsky and C. M. Lieber, Mater. Today **8**, 20 (2005).
[4] B.-K. Kim, J.-J. Kim, J.-O. Lee, K. -J. Kong, H. J. Seo, and C. J. Lee, Phys. Rev. B **71**, 153313 (2005).
[5] L. J. Lauhon, M. S. Gudiksen, D. Wang, and C. M. Lieber, Nature (London) **420**, 57 (2002).
[6] Y. Zhang, R. E. Russo, and S. S. Mao, Appl. Phys. Lett. **87**, 043106 (2005).
[7] H.-J. Choi*et al.*, J. Phys. Chem. B **107**, 8721 (2003).
[8] O. Hayden, A. B. Greytak, and D. C. Bell, Adv. Mater. (Weinheim, Ger.) **17**, 701 (2005).
[9] R. Könenkamp, R. C. Word, and C. Schlegel, Appl. Phys. Lett. **85**, 6004 (2005).
[10] L. J. Lauhon, M. S. Gudiksen, and C. M. Lieber, Philos. Trans. R. Soc. London, Ser. A **362**, 1247 (2004).
[11] E. Ertekin, P. A. Greaney, D. C. Chrzan, and T. D. Sands, J. Appl. Phys. **97**, 114325 (2005).
[12] M. Yu. Gutkin, I. A. Ovid'ko, and A. G. Sheinerman, J. Phys.: Condens. Matter **12**, 5391 (2000).
[13] S. Raychaudhuri and E. T. Yu, J. Appl. Phys. **99**, 114308 (2006).
[14] J. W. Matthews, J. Vac. Sci. Technol. **12**, 126 (1975).
[15] J. Y. Tsao, *Materials Fundamentals of Molecular Beam Epitaxy* (Academic, San Diego, 1993), pp. 151–168.
[16] J. F. Nye, *Physical Properties of Crystals* (Oxford University Press, Oxford, 1985), pp. 82–104, 131–142.
[17] J. P. Hirth and J. Lothe, *Theory of Dislocations* (McGraw-Hill, New York, 1968), pp. 29–56, 140–144, 254–265, 288–307, 355–562, 411–432.
[18] H. -M. Lin*et al.*, Nano Lett. **3**, 537 (2003).
[19] J. A. Floro, D. M. Follstaedt, P. Provencio, S. J. Hearne, and s. R. Lee, J. Appl. Phys. **96**, 7087 (2004).
[20] *Group IV Elements, IV-IV and III-V Compounds*, Landolt-Börnstein, Group III, Vol. 41, Part A (Springer, Berlin, 2001).
[21] S. Takeuchi and K. Suzuki, Phys. Status Solidi A **171**, 99 (1999).
[22] O. Ambacher *et al.*, J. Phys.: Condens. Matter **14**, 3399 (2002).